Neuroradiology (2020) 62:1285–1292
https://doi.org/10.1007/s00234-020-02466-0

SPINAL NEURORADIOLOGY

Detection of the common origin of the radiculomedullary artery with the feeder of spinal dural arteriovenous fistula using slab maximum intensity projection image

Masafumi Hiramatsu[1] · Kenji Sugiu[1] · Takao Yasuhara[1] · Tomohito Hishikawa[1] · Jun Haruma[1] · Yu Takahashi[1] · Satoshi Murai[1] · Kazuhiko Nishi[1] · Yoko Yamaoka[1] · Isao Date[1]

Received: 9 March 2020 / Accepted: 22 May 2020 / Published online: 2 June 2020

Abstract

Purpose Endovascular therapy to the spinal dural arteriovenous fistula (SDAVF) with a common origin of the radiculomedullary artery and the feeder of the shunt has the risk of spinal cord infarction. This study aimed to retrospectively assess the detection rate of normal spinal arteries from the feeder of SDAVF.

Methods We retrospectively collected the angiographic and clinical data of SDAVFs. This study included 19 patients with 20 SDAVF lesions admitted to our department between January 2007 and December 2018. We assessed the detection rate of normal radiculomedullary artery branched from the feeder of SDAVF between the period using the image intensifier (II) and flat panel detector (FPD) and evaluated the treatment results.

Results The detection rates of the radiculomedullary artery branched from the feeder of SDAVF were 10% (1/10 lesions) during the II period and 30% (3/10 lesions) during the FPD period. During the FPD period, all normal radiculomedullary arteries branched from the feeder were only detected on slab maximum intensity projection (MIP) images of rotational angiography, and we could not detect them in 2D or 3D digital subtraction angiography. All lesions that had a common origin of a normal radiculomedullary artery and the feeder were completely obliterated without complications. There was no recurrence during the follow-up period.

Conclusions The flat panel detector and slab MIP images seem to show the common origin of the normal radiculomedullary arteries from the feeder more accurately. With detailed analyses, SDAVF can be safety treated.

Keywords Slab MIP image · Spinal dural arteriovenous fistula · Radiculomedullary artery · Spinal artery

Abbreviations

AKA	Adamkiewicz's artery
ARMedA	anterior radiculomedullary artery
ASA	anterior spinal artery
EVT	endovascular therapy
FPD	flat panel detector
II	image intensifier
PRMedA	posterior radiculomedullary artery
NBCA	n-butyl-cyanoacrylate
PSA	posterolateral spinal artery
SDAVF	spinal dural arteriovenous fistula
2D-DSA	two-dimensional DSA
3D-DSA	three-dimensional DSA

Presentation at meeting The abstract of this article was presented in whole at the 15th congress of World Federation of Interventional and Therapeutic Neuroradiology.

✉ Masafumi Hiramatsu
mhiramatsu@okayama-u.ac.jp

[1] Department of Neurological Surgery, Okayama University Graduate School of Medicine, Dentistry and Pharmaceutical Sciences, 2-5-1 Shikata-cho, Kita-ku, Okayama 700-8558, Japan

Background

Spinal dural arteriovenous fistulas (SDAVFs) are rare with an assumed annual incidence of 5–10 cases per one million population [1] and are most frequent in the spinal arteriovenous shunt [2]. The treatment options for SDAVF consist of

endovascular therapy (EVT) and interruption of the draining vein using direct surgery [3–5]. Direct surgery can be invasive, but it can occlude the shunt robustly. Although EVT is less invasive and general anesthesia is not indispensable, the most important problem is the possibility of spinal infarction due to glue migration to the invisible spinal artery [6]. To avoid glue migration, it is necessary to detect the co-existing radiculomedullary artery connecting the spinal artery with the feeder of SDAVF. The purpose of this study is to assess the detection rate of the common origin of the normal radiculomedullary artery from the feeder of SDAVF.

Materials and methods

All procedures performed in studies involving human participants were in accordance with the ethical standards of our institutional research committee and with the 1964 Helsinki declaration and its later amendments. Written informed consent was obtained from all patients before DSA and treatment, but written informed consent for this study was not required because of the retrospective and noninvasive study design. Subjects consisted of 20 SDAVF lesions in 19 patients admitted to our department between January 2007 and December 2018 who exhibited myelopathy. We excluded spinal epidural AVF with intradural drainage. We made the diagnosis based on a previous study by Kiyosue et al. [7].

We examined the patient background (age, sex), characteristics of lesions (lesion level, symptom), angioarchitecture (feeder, draining vein, normal spinal artery), details of treatment (endovascular procedure, direct surgery), results of treatment, and results of follow-up (recurrence, complete occlusion on the final evaluation).

Preoperative examination

In our department, DSA of the segmental arteries was performed under local anesthesia in all patients in which SDAVF was suspected based on their medical history and MRI findings. After a 4-Fr sheath insertion to the femoral artery, routine heparinization (intravenous bolus injection of 2000 U) is performed for all patients. Two-dimensional DSA (2D-DSA) of the thoracic and lumbar segmental arteries was conducted to search for the feeder and the spinal arteries. Three-dimensional (3D) DSA was performed to feeder. With the patient holding their breath, rotational imaging with a 5-s protocol was consecutively conducted twice to obtain mask and contrast-enhanced images. For 3D-DSA, a 4-Fr diagnostic catheter was inserted into a target segmental artery, and a 100% iodine contrast medium with 300-mg/mL concentration was infused using an injector (0.8–1.0 mL/s flow rate, 1.5–2.0 s delay, 5.0–7.0 mL total).

In our department, an image intensifier (II) was used to acquire 2D- and 3D-DSA images until March 2013. After April 2013, a flat panel detector (FPD) was used. After obtaining 3D-DSA images with an FPD, we reconstructed slab maximum intensity projection (MIP) images in order to analyze the detailed angioarchitecture.

An Axiom Artis BA (Siemens Healthcare GmbH, Forchheim, Germany) was used as an II. During the 5-s run, the rotation angle is 200° with a 1.5° increment, revealing 133 projections with a matrix of 1024 × 1024 image elements. The active imaging size was 13.1 mm × 13.1 mm for 1024 × 1024 pixels, the digitization depth was 12 bit, and the pixel pitch was 12.8 mm. The following imaging conditions were adopted: 3D acquisition: 70 kV, 10 ms, small focal spot, 0.36 μGy/frame, Sub/Nat Mask Recon.: 256 × 256 matrix, 0.35–0.55 mmSL. Bone, Auto. Workstation: LEONARDO workstation (Siemens Healthcare).

An Artis zee biplane (Siemens Healthcare) was used as an FPD. During the 5-s run, the rotational angle is 200° with a 1.5° increment, revealing 133 projections with a matrix of 1024 × 1024 image elements. The active imaging size was 382 × 293 mm for 2480 × 1920 pixels, the digitization depth was 16 bit, and the pixel pitch was 154 μm. The following imaging conditions were adopted: 3D acquisition: 70 kV, 12.5 ms, small focal spot, 0.36 μGy/frame, Sub/Nat Mask Recon.: 512 × 512 matrix, 0.22–0.34 mmSL. Hounsfield units, Auto. Workstation: *syngo* X Workplace (Siemens Healthcare).

Anatomical classification and terminology

We used anatomical classification which was supposed by Thron AK as follows [8]. The anterior radiculomedullary arteries (ARMedA), in which the persistent medullary branch was running with the anterior nerve root to join the longitudinal trunk, were termed the anterior spinal artery (ASA). The posterior radiculomedullary arteries (PRMedA), in which the persistent medullary branch accompanies the posterior nerve root and joins the longitudinal systems on the posterolateral aspect of the spinal cord, were called the posterolateral spinal artery (PSA).

Treatment

Direct surgery was selected in principle when preoperative examination revealed the common origin of the normal spinal artery related to the feeder. When there was no normal spinal artery related to the feeder, an EVT was selected as a first choice. When shunt obliteration was not achieved, or when recurrence was noted after EVT, direct surgery was additionally performed.

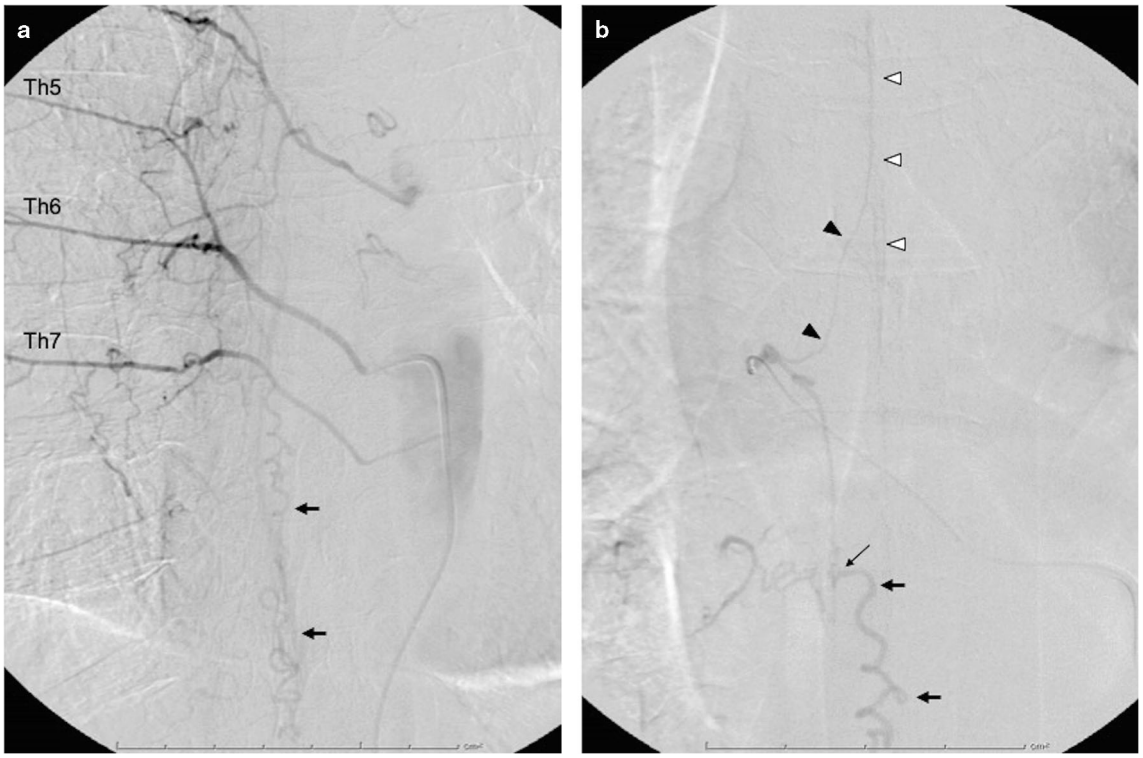

Fig. 1 A 63-year-old female with dural arteriovenous fistula (SDAVF) presented with gait disturbance for 2 months. **a** The A-P view of the spinal angiograph of the right Th6 segmental artery shows draining vein (black large arrow) of SDAVF. The right Th5 segmental artery has a common origin with the right Th6 segmental artery. The right Th4 and Th7 segmental arteries are visualized via collateral flow. **b** The A-P view of superselective angiography via microcatheter in the right Th6 segmental artery shows shunt point (black arrow), draining vein (black large arrow), anterior radiculomedullary artery (black arrowhead), and anterior spinal artery (white arrowhead)

For direct surgery, coagulation and disconnection of an intradural draining vein were performed. For EVT, a 4-Fr catheter was inserted into the segmental artery as a guiding catheter under local anesthesia. After inserting a microcatheter into the feeder as distal as possible, diluted n-butyl-2-cyanoacrylate (NBCA) was injected. We determined the concentration of NBCA according to the lesion characteristics and the position of the microcatheter with the shunt point. Usually, the concentration of NBCA is 15 to 30%. We attempted to penetrate the NBCA into an intradural draining vein but stopped when the reflux of the NBCA into a proximal to the catheter was noted.

Follow-up

Follow-up was conducted at the outpatient clinic of our department. When neurological examination and MRI suggested recurrence, the patient was admitted in order to evaluate the recurrence using DSA.

Assessment

We assessed the detection rate of the common origin of the normal spinal artery with the feeder of the SDAVF between the II and the FPD period. Furthermore, we divided the participants into two groups as follows: group A was SDAVF with a common origin and group B was SDAVF without a common origin. We evaluated the treatment results of groups A and B.

Statistical analyses

For statistical analyses, JMP10 software (SAS Institute Inc., Cary, NC, USA) was used. Descriptive statistics are expressed as the mean with standard deviation and categorical variables as numbers and percentages.

Results

Lesion characteristics

The mean age of the patients was 66 years (range: 55–84 years), and the majority of patients were men (85%). In all patients, myelopathy was the primary symptom, and T2-weighted MRI showed high-intensity signals in the spinal cord. Flow voids were observed in 13 lesions (65%), and in all lesions, all feeders were the radiculomeningeal artery. Ipsilateral multiple feeders were found in three lesions (15%), and there are no bilateral feeders.

Detection rate of the normal spinal artery

The detection rates of the common origin of the normal radiculomedullary artery with a feeder were 10% (1/10) during the II period and 30% (3/10) during the FPD period. In one case during the II period, the ARMedA from the feeder was only detected by superselective DSA via a microcatheter just before the embolization, and we could not detect the ARMedA from the other segmental arteries (Fig. 1). During the FPD period, the ARMedA from the feeder was detected in one case (Fig. 2), and the PRMedA from the feeder was detected in two cases. All normal radiculomedullary arteries from the feeders were only detected by slab MIP images during FPD period. We could not identify the normal spinal artery from the feeder by usual 2D-DSA or volume-rendering 3D-DSA images during both periods. Furthermore, in the case that detected ARMedA from the feeder, we detected an additional ARMedA from another segmental artery, which was considered the Adamkiewicz's artery (AKA), because the vessel had a larger diameter than that of the feeder (Fig. 2).

The distribution of both shunt level and the origin of all normal ARMedA-ASA is described in Fig. 3. The shunt level ranged from Th5 to L1 (most frequent level: Th6), and 10 lesions (50%) were from the left side. We could not find a normal ARMedA connected to the ASA in one patient during the II period. And we detected 24 ARMedA-ASA in 18 patients, 21 (88%) of which were from the left side. The level of segmental arteries branching normal ARMedA ranged from Th5 to L2 (most frequent level: Th6). The distribution of shunt levels and that of ARMedA overlapped.

Treatment and follow-up results

In group A (with a common origin), direct surgery was selected for three patients, and EVT was selected for one patient with multiple feeders as curative treatment (Fig. 4). All lesions were completely obliterated without complication and showed no recurrence for the follow-up period. The median (IQR) follow-up period was 9 (4–19) months.

In group B (without a common origin), 13 lesions were treated with EVT as the first treatment, and 8 lesions were completely obliterated by EVT only. Seven lesions were completely obliterated by direct surgery. One morbidity (6%) occurred due to delayed venous thrombosis after successful EVT. All obliterated lesions showed no recurrence for the follow-up period. The median (IQR) follow-up period was 35 (5–77) months.

Discussion

We have demonstrated the difference in detection rates of the common origin of a normal spinal artery from the feeder of SDAVF between the II and the FPD periods. Furthermore, we revealed that the treatment results, mainly by direct surgery, were not inferior in SDAVF with a common origin if we could appropriately identify the normal spinal artery from the feeder of SDAVF. EVT could be considered in particular cases.

Fig. 2 An 80-year-old male with dural arteriovenous fistula (SDAVF) presented with motor and sensory disturbance of the lower extremities. **a** The A-P view of the spinal angiograph of the left Th9 segmental artery shows a normal anterior radiculomedullary artery (ARMedA: black arrowhead) and ASA (white arrowhead). **b** The A-P view of the spinal angiograph of the left Th6 segmental artery shows shunt point (black arrow) and intradural drainage (black large arrow) of SDAVF. **c** The A-P view of the 3D-DSA of the left Th6 segmental artery show shunt point (white arrow) and intradural drainage (white large arrow) of SDAVF. **e**, **f** The coronal view (**d**, **e**) and sagittal view (**f**) of the slab MIP images of the left Th6 segmental artery show shunt point (white arrow) and intradural drainage (white large arrow) of the SDAVF, ARMedA (black arrowhead), and ASA (white arrowhead). **g**, **h** The A-P view (**g**) of the spinal angiograph and the coronal view of the slab MIP image (**h**) of the left Th6 segmental artery after direct surgery of SDAVF show ARMedA (black arrowhead) and ASA (white arrowhead) without SDAVF

Detection rate of the spinal artery

Lasjaunias et al. reported that the number of ARMedAs in the thoracic level was 2 to 3 and that of the PRMedAs was 6 to 9 [9]. The origin of the artery of the lumbar enlargement, so-called AKA, originates from Th9 to Th12 in 75% of cases and is more common on the left side. In contrast, the detection number of the ARMedA is relatively low using imaging modalities such as CTA, intra-arterial CTA, and contrast-enhanced MRA. Using CTA, the detection rate of AKA was 60–90% [10, 11], while using intra-arterial CTA, it was 94–100% [12]. However, these studies could only detect one ARMedA in each case, and there can be other several ARMedAs and PRMedAs.

The majority of the SDAVF occurs at the thoracic spine, especially at Th5 to L1 [3, 7, 13]. This common site of SDAVF overlaps the common site of AKA described above. Therefore, the common origin of a normal radiculomedullary artery with a feeder can sometimes occur. Several case reports have described the common origin of SDAVF and the normal spinal artery, the majority of which were SDAVF that shared an arterial origin with the AKA; these spinal arteries are large enough to recognize on conventional 2D-DSA [14–19]. Aggarwell et al. reported that superselective angiography revealed AKA more clearly [14], and Shapiro reported that DynaCT MIP images showed the origins of the feeder and ARMedA [18]. Some larger case series reported that the incidence of the common origin of the ARMedA and the feeder of the SDAVF was 1% to 14% [5, 6, 20, 21], but these studies detected the common origin using conventional angiographic data. Adrianto et al. observed the concomitant origin of the ASA or PSA with the feeder of an SDAVF and reported that a

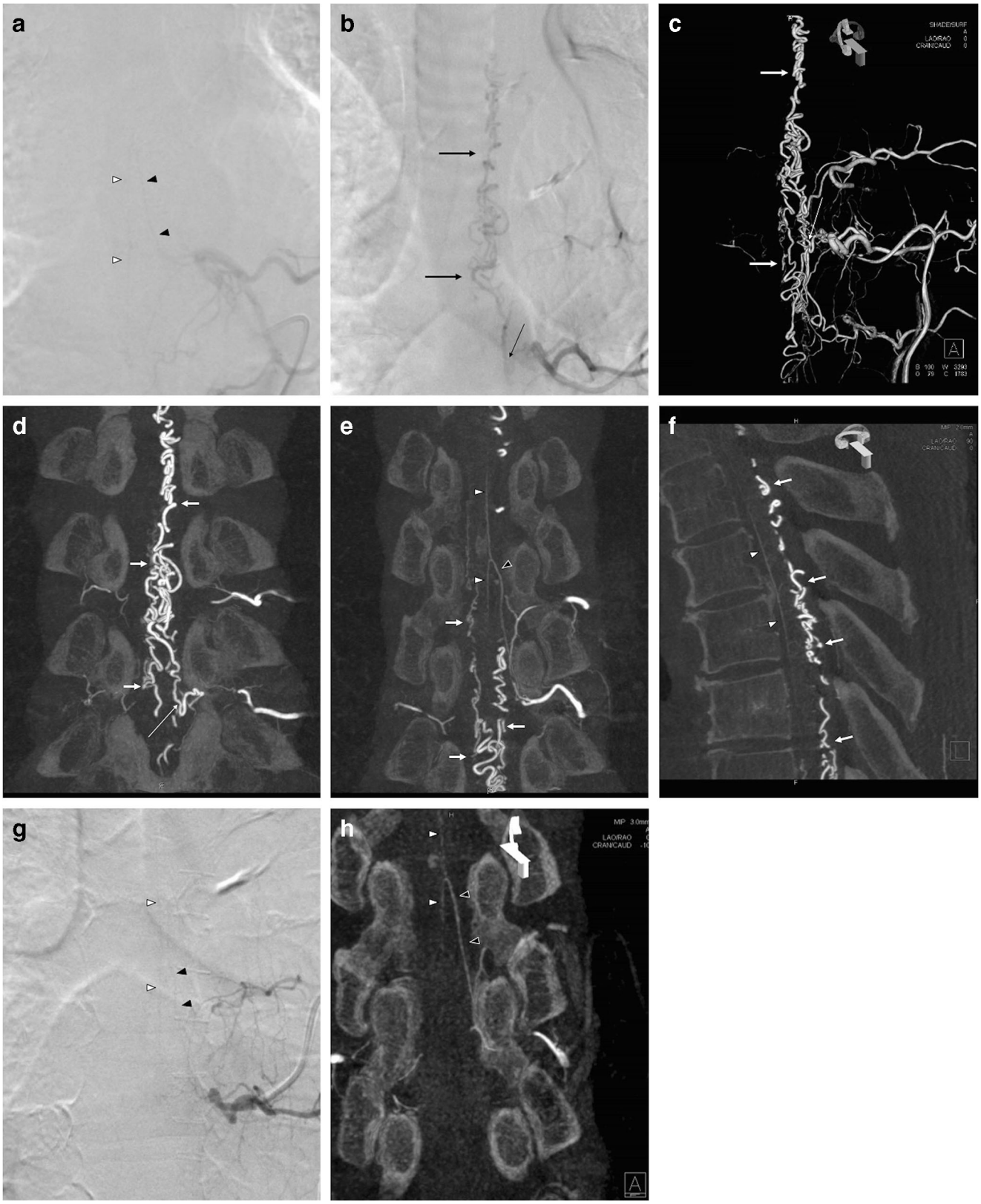
a
b
c
d
e
f
g
h

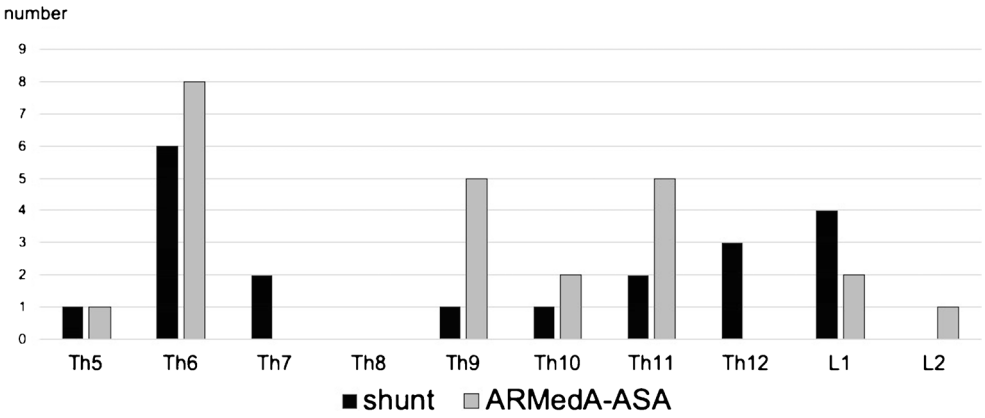

Fig. 3 The distribution of both the shunt level and the origin of the normal ARMedA-ASA. Note that both distributions are overlapping. ARMedA: anterior radiculomedullary artery, ASA: anterior spinal artery

concomitant origin occurs occasionally (14%) [21]. Furthermore, other case series did not report the detection rate of the spinal artery from the feeder [3, 4].

We report that the detection rate of the common origin was increased from 10% during the II period to 30% during the FPD period. Furthermore, throughout the study period, we could not detect the spinal artery using the usual 2D- or volume rendering image of 3D-DSA. We considered that the noisy lesion characteristics of the SDAVF superimposed and concealed the normal fine angioarchitecture. Of course, there can be cases in which we can visualize the common origin of large normal radiculomedullary arteries branched from the feeder by 2D- or usual 3D-DSA images, not only slab MIP images. Furthermore, we can easily change image quality by adjustment of the window level or width. Although adjustment of 3D-DSA may be able to visualize tiny vessels, image quality differs depending on lesion characteristics, operators, and image display.

In this regard, other methodologies are necessary to visualize normal fine angioarchitecture, such as DSA under general anesthesia, superselective DSA using microcatheter, or reconstruction of slab MIP images [7, 22]. In this report, we revealed that the slab MIP image can visualize normal fine angioarchitecture clearly without the need for additional invasive procedures. This is the first report to demonstrate the improvement of the detection rate by the renewal of imaging modality and the importance of slab MIP images.

Treatment strategy

Similarly to other institutions, we believe that the common origin of the normal spinal artery and a feeder of SDAVF is a contraindication for EVT to avoid glue migration to the spinal artery; therefore, we selected direct surgery in principle in these cases [6, 20]. Exceptionally, if the lesion has multiple feeders, and one of the feeders has a common origin, we will try EVT with meticulous care based on detailed analyses of lesions. Specifically, after proximal occlusion of the feeder, which has a common origin, using coils or large particles at first, we will attempt to penetrate the NBCA to the shunt lesion from other feeders (Fig. 4). Under these strategies, we can completely occlude these lesions without complication.

Limitation

The current study has some limitations. First, this was a retrospective study. Second, the number of patients was small. Third, this is not the comparative study of imaging modalities for the same study population, and image acquiring techniques between two groups have some differences (equipment, workstation, and reconstruction protocol) which can lead to bias. Fourth, we did not obtain the DSA data under general anesthesia. Fifth, we did not confirm the spinal artery using a provocation test or temporary clipping of the visualized spinal artery. In the future, a prospective observational study with a large number of patients should be performed.

Fig. 4 A 51-year-old male with dural arteriovenous fistula (SDAVF) presented with sensory disturbance of the lower extremities. **a** Fusion image of the 3D-DSA of the right Th5–7 shows SDAVF and intradural drainage (white large arrow). **b**, **c** The coronal view of the slab MIP images of the right Th5 (**b**) and the right Th6 (**c**) segmental artery shows shunt point (white arrow) and intradural drainage (white large arrow) of SDAVF. **d** The coronal view of the slab MIP image of the right Th7 segmental artery shows the shunt point (white arrow), intradural drainage (white large arrow) of SDAVF, posterior radiculomedullary artery (black arrowhead), and posterolateral spinal artery (white arrowhead). **e**, **f** The A-P view of the spinal angiograph of the right Th7 segmental artery before (**e**) and after (**f**) embolization using particulate material. After embolization, the feeder (black arrow) and shunt flow from the right Th7 segmental artery disappear. **g** Oblique view of the spinal angiograph of the right Th6 segmental artery before embolization showed the shunt point (black arrow). **h** Cast (black circle) of n-butyl-2-cyanoacrylate (NBCA) after embolization of the right Th6 and 7 segmental arteries with NBCA. Note that NBCA is penetrated to the draining vein via the shunt point (black arrow) shown in **g**. After embolization, the shunt is obliterated (not shown)

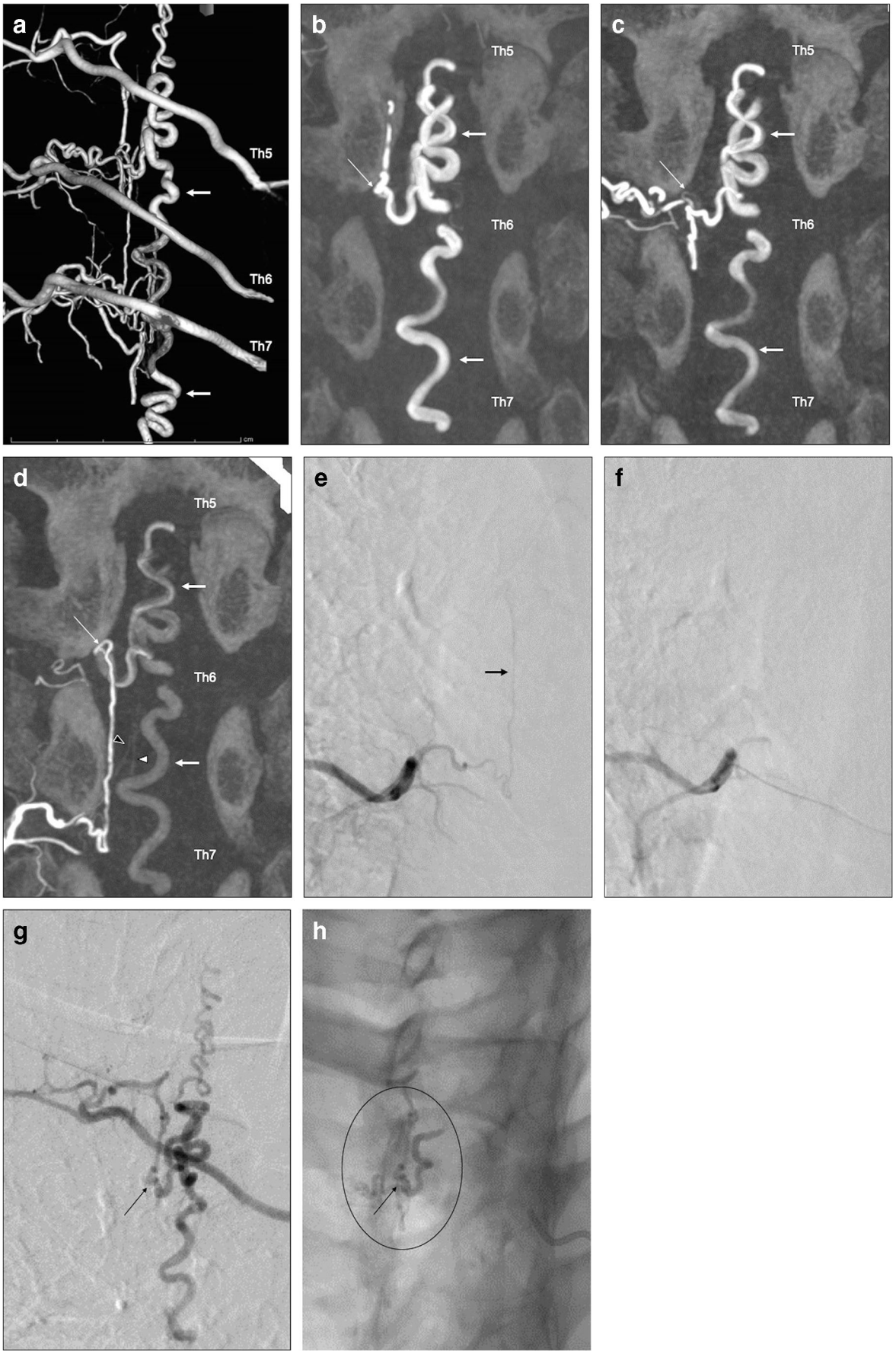
a
Th5
Th6
Th7
b
Th5
Th6
Th7
c
Th5
Th6
Th7
d
Th5
Th6
Th7
e
f
g
h

Conclusions

The flat panel detector and slab MIP images seem to show the common origin of the normal spinal arteries from the feeder more accurately. Further evaluation is needed to prove the usefulness of slab MIP images. SDAVF can be safely treated by using detailed analyses.

Acknowledgments We thank Mr. Niida N (Siemens Healthcare) for his technical support with the reconstruction method of three-dimensional rotational angiography.

Funding information The authors have not received any research grant nor funding.

Compliance with ethical standards

Conflict of interest The authors declare that they have no conflict of interest.

Ethics approval The study protocol was approved by the Ethics Review Board of our hospital.

Informed consent For this type of study, formal consent is not required.

Consent for publication For this type of study, formal consent is not required.

References

1. Thron A (2001) Spinal durale arteriovenose fisteln. Radiologe 41: 955–960
2. Spetzler RF, Detwiler PW, Riina HA, Porter RW (2002) Modified classification of spinal cord vascular lesions. J Neurosurg 96:145–156
3. Koch MJ, Stapleton CJ, Agarwalla PK, Torok C, Shin JH, Coumans JV, Borges LF, Ogilvy CS, Rabinov JD, Patel AB (2017) Open and endovascular treatment of spinal dural arteriovenous fistulas: a 10-year experience. J Neurosurg Spine 26:519–523
4. Saladino A, Atkinson JLD, Rabinstein AA, Piepgras DG, Marsh WR, Krauss WE, Kaufmann TJ, Lanzino G (2010) Surgical treatment of spinal dural arteriovenous fistulae: a consecutive series of 154 patients. Neurosurgery 67:1350–1357
5. Sasamori T, Hida K, Yano S, Asano T, Seki T, Houkin K (2016) Long-term outcomes after surgical and endovascular treatment of spinal dural arteriovenous fistulae. Eur Spine J 25:748–754
6. Gokhale S, Khan SA, McDonagh DL, Britz G (2014) Comparison of surgical and endovascular approach in management of spinal dural arteriovenous fistulas: a single center experience of 27 patients. Surg Neurol Int 5:7
7. Kiyosue H, Matsumaru Y, Niimi Y, Takai K, Ishiguro T, Hiramatsu M, Tatebayashi K, Takagi T, Yoshimura S, JSNET Spinal AV Shunts Study Group (2017) Angiographic and clinical characteristics of thoracolumbar spinal epidural and dural arteriovenous fistulas. Stroke 48:3215–3222
8. Thron AK (2016) Vascular anatomy of the spinal cord, radioanatomy as the key to diagnosis and treatment, Second Edition. Springer, Switzerland, p 15
9. Lasjaunias P, Berenstein A, terBrugge KG (2001) Spinal artery. Surgical neuroangiography 1, clinical vascular anatomy and variations, Second edition. Springer-Verlag, Berlin, p 123
10. Takase K, Akasaka J, Sawamura Y, Ota H, Sato A, Yamada T, Higano S, Igarashi K, Chiba Y, Takahashi S (2006) Preoperative MDCT evaluation of the artery of Adamkiewicz and its origin. J Comput Assist Tomogr 30:716–722
11. Yoshioka K, Niinuma H, Ehara S, Nakajima T, Nakamura M, Kawazoe K (2006) MR angiography and CT angiography of the artery of Adamkiewicz: state of the art. RadioGraphics 26:S63–S73
12. Uotani K, Yamada N, Kono AK, Taniguchi T, Sugimoto K, Fujii M, Kitagawa A, Okita Y, Naito H, Sugimura K (2008) Preoperative visualization of the artery of adamkiewicz by intra-arterial CT angiography. AJNR Am J Neuroradiol 29:314–318
13. Gemmete JJ, Chaudhary N, Elias AE, Toma AK, Pandey AS, Parker RA, Davagnanam I, Maher CO, Brew S, Robertson F (2013) Spinal dural arteriovenous fistulas: clinical experience with endovascular treatment as a primary therapy at 2 academic referral centers. AJNR Am J Neuroradiol 34:1974–1979
14. Aggarwal S, Willinsky R, Montanera W, Terbrugge K, Wallace MC (1992) Superselective angiography of a spinal dural arteriovenous fistula having a common segmental origin with the artery of Adamkiewicz. Neuroradiology 34:352–354
15. Cawley CM, Howard BM, Barrow DL (2019) Microsurgical management of a spinal dural arteriovenous fistula with shared blood supply to the artery of Adamkiewicz: 3-dimensional operative video. Oper Neurosurg (Hagerstown) 16:E174–E175
16. Eneling J, Karlsson PM, Rossitti S (2014) A treatment-refractory spinal dural arteriovenous fistula sharing arterial origin with the artery of Adamkiewicz: repeated endovascular treatment after failed microsurgery. Surg Neurol Int 5:S165–S169
17. Hadzipasic M, Grant R, Johnson M, Cheng J, Bulsara KR (2017) Spinal dural arteriovenous fistulas with segmental arterial supply also giving rise to a radiculomedullary artery: a case report and review of the literature. World Neurosurg 97:E21–E26
18. Shapiro M, Kister I, Raz E, Loh J, Young M, Goldman-Yassen A, Chancellor B, Nelson PK (2019) Spinal dural fistula and anterior spinal artery supply from the same segmental artery: case report of volumetric T2 MRI diagnosis and rational endovascular treatment. Interv Neruroradiol 25:579–584
19. Shedid D, Podichetty VK (2009) Common origin of the artery of adamkiewicz and a posterior spinal artery with a spinal dural arteriovenous fistula: a case report. Br J Neurosurg 23:630–633
20. Kirsch M, Berg-Dammer E, Musahl C, Bäzner H, Kühne D, Henkes H (2013) Endovascular management of spinal dural arteriovenous fistulas in 78 patients. Neuroradiology 55:337–343
21. Adrianto Y, Yang KH, Koo HW, Park W, Jung SC, Park JE, Kim KK, Jeon SR, Suh DC (2017) Concomitant origin of the anterior or posterior spinal artery with the feeder of a spinal dural arteriovenous fistula (SDAVF). J Neurointerv Surg 9:405–410
22. Aadland TD, Thielen KR, Kaufmann TJ, Morris JM, Lanzino G, Kallmes DF, Schueler BA, Cloft H (2010) 3D c-arm conebeam CT angiography as an adjunct in the precise anatomic characterization of spinal dural arteriovenous fistulas. AJNR Am J Neuroradiol 31: 476–480